

Solvent-free polymer electrolytes based on thermally annealed porous P(VdF-HFP)/P(EO-EC) membranes

Jae-Deok Jeon^a, Byung-Won Cho^b, Seung-Yeop Kwak^{c,*}

^a *Research Institute of Advanced Materials (RIAM), and School of Materials Science and Engineering, Seoul National University, San 56-1, Sillim-dong, Gwanak-gu, Seoul 151-744, South Korea*

^b *Eco-Nano Research Center, Korea Institute of Science and Technology (KIST), P.O. Box 131, Cheongryang, Seoul 130-650, Korea*

^c *Hyperstructured Organic Materials Research Center (HOMRC), and School of Materials Science and Engineering, Seoul National University, San 56-1, Sillim-dong, Gwanak-gu, Seoul 151-744, South Korea*

Received 17 November 2004; accepted 15 December 2004

Available online 29 January 2005

Abstract

Highly porous membranes composed of poly(vinylidene fluoride-co-hexafluoropropylene) [P(VdF-HFP)] and poly(ethylene oxide-co-ethylene carbonate) [P(EO-EC)] were prepared by a phase inversion method. The existence of viscous P(EO-EC) in the membranes not only contributed to the flexibility and high porosity but also led to a decrease in the mechanical strength. In an attempt to enhance the mechanical properties of porous membranes, a thermal annealing technique was considered a promising approach. When the membranes were annealed at 110 °C for 2 h in an ordinary vacuum oven, they showed a highly ordered pore structure (i.e., honeycomb-like structure) and had a smaller pore size than unannealed membranes. This contributed to enhancement of mechanical strength in the membranes. Instead of organic solvent, viscous P(EO-EC) complexed with LiCF₃SO₃ was added to the pores of annealed and unannealed membranes, thereby producing solvent-free polymer electrolytes. Polymer electrolytes based on annealed membranes exhibited a high uptake value of the P(EO-EC)/LiCF₃SO₃ mixture and had a maximum conductivity value of $3.5 \times 10^{-5} \text{ S cm}^{-1}$ at room temperature, which is similar to that of unannealed membrane-based polymer electrolytes. Their conductivities were observed to increase with increasing P(EO-EC) content in the membranes due to this high uptake. Considering the foregoing facts, the mechanical properties of porous membranes can be improved by the thermal annealing without risking any deterioration of porosity, uptake, and electrochemical performance.

© 2005 Elsevier B.V. All rights reserved.

Keywords: Solvent-free polymer electrolyte; Porous membrane; Thermal annealing; Rechargeable lithium batteries

1. Introduction

Ion-conducting polymer electrolytes have contributed to the development of lithium battery technology by replacing the liquid electrolyte and thereby enabling the fabrication of flexible, compact, and laminated solid-state structures free from leaks of the electrolyte [1]. Among these, solvent-free polymer electrolytes (SPEs) formed by complexes of

a lithium salt (LiX) with a polyether such as poly(ethylene oxide) (PEO) have received considerable attention due to their advantages in terms of the ease of fabrication, flexibility in dimensions, good mechanical properties, safety features, and excellent stability at the lithium interface [2–5]. However, their low ionic conductivities have been the reason for them not being used in practical applications in rechargeable lithium batteries that require a value of above $10^{-4} \text{ S cm}^{-1}$ at room temperature.

The ion transport of the SPEs is induced via their rapid segmental motion combined with strong Lewis acid–base in-

* Corresponding author. Tel.: +82 2 8808365; fax: +82 2 8851748.
E-mail address: sykwak@snu.ac.kr (S.-Y. Kwak).

teractions between the cation and the donor atom present in the amorphous phase. In addition, it was initially assumed that an ion transport mechanism is associated with crystalline domains because ions move along the PEO helices. However, it was soon established that ion transport only occurs in the amorphous regions of the materials, associated with polymer segmental motion [6]. Therefore, most approaches for enhancing the conductivity of PEO systems are focused on lowering the degree of PEO crystallinity or reducing the glass transition temperature, T_g , through the modification of the polymer structures [7,8] and the incorporation of plasticizers [9–11] or ceramic fillers [12–14].

The highest conductivity of ca. $10^{-3} \text{ S cm}^{-1}$, which is close to that of liquid electrolytes, was achieved by gel polymer electrolytes (GPEs). GPEs encapsulate a large amount of organic solvent such as ethylene carbonate (EC) and propylene carbonate (PC) into the porous structure of polymer host, resulting in useful conductivity values of over $10^{-4} \text{ S cm}^{-1}$. This has met with success but still has some drawbacks such as the addition of organic solvent promotes deterioration of the mechanical properties of electrolytes and increases its reactivity towards the lithium metal anode [5,15]. These systems also retain a significant volume of the volatile liquid trapped in the gel pores, resulting in a large increase in vapor pressure as the temperature is raised. Lastly, the sealing of battery cells still remains a problem. Therefore, only SPEs with high ionic conductivity can ensure an efficient performance.

Our strategy in developing solvent-free polymer electrolytes for rechargeable lithium batteries is as follows. First, poly(ethylene oxide-co-ethylene carbonate) [P(EO-EC)] is synthesized using EC, which is normally used as organic solvent in GPEs. Due to the high polarity of carbonate groups linked by ether moieties, the dielectric constant of the P(EO-EC) and free ion content in the polymer electrolyte should be higher than those of PEO-based systems. These polar subunits also help reduce the crystallinity of the polymer. Then, porous membranes consisting of poly(vinylidene fluoride-co-hexafluoropropylene) [P(VdF-HFP)] and P(EO-EC) are conveniently obtained by a phase inversion method, which is known to be effective for producing a porous structure. The introduction of P(EO-EC) into the membranes improves their flexibility and produces larger pore sizes than the pure P(VdF-HFP) membrane. However, it also leads to the deterioration of the mechanical strength of the membranes. Among the various methods that can be used to overcome this shortcoming, we proposed the thermal annealing technique in this study. Viscous P(EO-EC) complexed with Li-salt is filled into the pores of porous membranes, thereby producing solvent-free polymer electrolytes. This method provides a new approach for preparing polymer electrolytes that combine both the concepts of SPEs and GPEs. In this study, we focused on solvent-free polymer electrolytes based on annealed and unannealed porous membranes, and their characteristics and performance are presented and discussed herein.

2. Experimental

2.1. Preparation of porous membranes and polymer electrolytes

P(EO-EC) was synthesized through ring opening polymerization. After 1 mol of EC (Aldrich Chemicals) as a monomer and 1 mmol of potassium methoxide (CH_3OK , Aldrich Chemicals) as an initiator were added to an argon-purged three-neck 250 mL round-bottomed flask, the mixture was stirred at 180°C for 15 h. Next, in order to remove the monomer, which remained the reaction mixture was dissolved in ethanol (200 mL) and the resulting solution was poured into ether (2 L). Viscous polymer precipitated while the monomer was dissolved in ether. After the ether layer was decanted from the solution, the resulting polymer was washed with ether several times until no monomer was left in the polymer. Then it was dried under vacuum at 80°C for 2 days. In order to replace all the hydroxyl groups with chlorine atoms, 10 mL of thionyl chloride (SOCl_2) was added to the polymer and refluxed for 48 h under argon. The final polymer was dried in a vacuum oven at 100°C for 24 h in order to remove all the volatile components and then was stored in a glove box.

Porous membranes were prepared by a phase inversion method. P(VdF-HFP) ($M_w = 4.6 \times 10^5$, Aldrich Chemicals) and P(EO-EC) were dissolved by stirring at 50°C for 5 h into the mixture of volatile solvent (acetone) and non-solvent (ethylene glycol). To prepare porous membranes with structural rigidity and high uptake of electrolyte materials, the weight ratio of polymers, solvent and non-solvent was optimized at 10:80:10. The composition of polymers was [(10 - x)wt% P(VdF-HFP): x wt% P(EO-EC)] where $x = 0, 1, 2, 3, 4,$ and 5 . When a completely homogenous mixture was obtained, the resulting viscous solution was cast with a doctor blade on a glass plate. Ethylene glycol was then removed by washing with methanol. After the solvent was allowed to slowly evaporate at room temperature, it was completely removed by heating under vacuum at 50°C for 24 h, thereby producing porous membranes. In order to improve the mechanical properties of the porous membranes, they were annealed at 110°C for 2 h in an ordinary vacuum oven. All porous membranes had a thickness of 180–190 μm .

To prepare polymer electrolytes, P(EO-EC) was first dissolved in acetone. When completely homogenous solution was obtained, an appropriate amount of lithium trifluoromethane sulfonate (LiCF_3SO_3 , Aldrich Chemicals) was added and then was further stirred until the Li-salt was completely dissolved. The resulting solution was left to evaporate the residual acetone under vacuum at 80°C . After perfect evaporation of the acetone, the porous membrane was filled for several times with the heated P(EO-EC)/ LiCF_3SO_3 mixture by using a vacuum filter equipment, thereby producing solvent-free polymer electrolytes. The mixture remaining on the surface was wiped with filter paper. In this study, M- V_xE_y and E- V_xE_y shall denote the porous Membrane with blend composition of P(VdF-HFP)/P(EO-EC) (x/y by wt%) and the

polymer Electrolyte filled with the P(EO-EC)/LiCF₃SO₃ inside pores of its membrane, respectively.

2.2. Characterization of porous membranes and polymer electrolytes

The chemical structure of synthesized P(EO-EC) was elucidated by ¹H NMR spectroscopy employing a Bruker DPX 300 spectrometer with the tetramethylsilane (TMS) proton signal as an internal standard in CDCl₃. The FT-IR spectra were recorded on a Perkin-Elmer GX IR spectrometer at room temperature by squeezing in a thin film between two plates of KBr. The molecular weights and molecular weight distribution were obtained using a Waters model 410 gel permeation chromatography instrument (GPC) connected to a Waters 410 differential refractometer. Three styragel columns connected in series were used with chloroform as solvent. The glass transition temperature of P(EO-EC) was determined by differential scanning calorimetry (DSC) with a TA instruments DSC 2920 at a heating rate of 10 °C min⁻¹ under nitrogen atmosphere.

The porosity of porous membranes was measured by immersing the membranes into *n*-butanol for 1 h and then calculated using the following equation

$$\text{porosity (\%)} = \frac{W_a/\rho_a}{W_a/\rho_a + W_p/\rho_p} \times 100 \quad (1)$$

where W_p is the weight of dry membranes, W_a is the weight of *n*-butanol absorbed in the wet membranes, ρ_a is the density of *n*-butanol and ρ_p is the density of membranes. The uptake of viscous P(EO-EC) was calculated by

$$\text{uptake (\%)} = \frac{W - W_o}{W} \times 100 \quad (2)$$

where W and W_o are the weights of the wet and dry membranes, respectively. Morphological examination of porous membranes was made by a field emission scanning electron microscope (FE-SEM, JEOL, JSM-6330F). The loss of electrolyte solution was measured from isothermal thermogravimetric analysis (TGA) plots. The polymer electrolytes were heated at 40 and 70 °C for 12 h under a flow of argon and the weight change was monitored as a function of time. Mechanical properties of porous membranes were measured at room temperature with a strain rate of 20 mm min⁻¹ according to the ASTM 882 procedure with a LLOYD LR10K universal testing instrument.

The ionic conductivity of polymer electrolytes was measured by the ac impedance technique in the temperature range of 5–95 °C and frequency range from 0.1 Hz to 1 MHz using a Zahner Elektrik IM6 impedance analyzer. The samples for conductivity measurements were prepared by sandwiching the polymer electrolytes between two 1.7 × 1.7 cm²-sized stainless steel (SS) electrodes. Each sample was allowed to equilibrate for 30 min at each temperature prior to taking measurement. All assemblies and testing operations of samples were performed in a dry room.

3. Results and discussion

3.1. Characteristics of P(EO-EC) copolymer

P(EO-EC) copolymer was synthesized by ring opening polymerization of EC. From the beginning of the reaction, gas (CO₂) was evolved vigorously from the reaction mixture and gas evolution continued for 15 h. Thus, the evolution of the CO₂ made some ethylene oxide units, thereby producing P(EO-EC) copolymer. It was reported [16] that the evolution of the CO₂ made entropy changes, ΔS_p , positive, so this polymerization became thermodynamically possible at high temperature. On the other hand, the color of the reaction mixture changed during the reaction. Initially, the reaction mixture was transparent liquid, but as soon as the reaction began, the color changed to light yellow (1–8 h), to darkened yellow (8–13 h), and finally to brown (>13 h). P(EO-EC) with hydroxyl end groups was replaced by non-reactive polar chlorine atoms since it reacts easily with lithium metal [17]. The resultant P(EO-EC) eventually became brown in appearance and very viscous.

The chemical structure of synthesized P(EO-EC) was studied by NMR. Fig. 1 shows the ¹H NMR spectra of the samples in CDCl₃. The singlet peak of EC is clearly observed at 4.54 ppm, but its peak becomes invisible after the polymerization for 15 h. Thus, the molar composition of P(EO-EC) can be calculated by comparing the area of the multiplet at 3.5–3.7 ppm, assigned to the ethylene oxide (EO) unit, with those of two triplets at 3.7 and 4.3 ppm, assigned to the ethylene carbonate (EC) unit. On the basis of the integrations obtained from ¹H NMR spectra, the monomer conversion and P(EO-EC) composition can be calculated as follows

$$\text{conversion (\%)} = \frac{A_b + A_c + A_d}{A_a + A_b + A_c + A_d} \times 100 \quad (3)$$

$$\text{EC content (mol\%)} = \frac{A_c + A_d}{A_b + A_c + A_d} \times 100 \quad (4)$$

$$\text{EO content (mol\%)} = 100 - \text{EC content (mol\%)} \quad (5)$$

where A_a , A_b , A_c , and A_d are the intensities of the a, b, c, and d proton peaks, respectively. From these results, we could confirm that monomer conversion was 100% and P(EO-EC) was a mixture of monomeric unit (EC units) and the corresponding EO units. Soga et al. [18] and several authors [19,20] reported that EC could be polymerized using Lewis acids, transesterification catalysts, or bases as initiators or catalysts. When Lewis acids or transesterification catalysts were used, the resultant polymers generally contained ca. 40–50 mol% of EC units (150–170 °C, 70–100 h). When bases were used, the resultant polymers contained ca. 10–20 mol% of EC units (ca. 150 °C, 72–98 h). In this study, EC was bulk polymerized by using CH₃OK as a base at 180 °C for 15 h, resulting in a P(EO-EC) copolymer consisting of ca. 30 mol% of EC units and ca. 70 mol% of EO units.

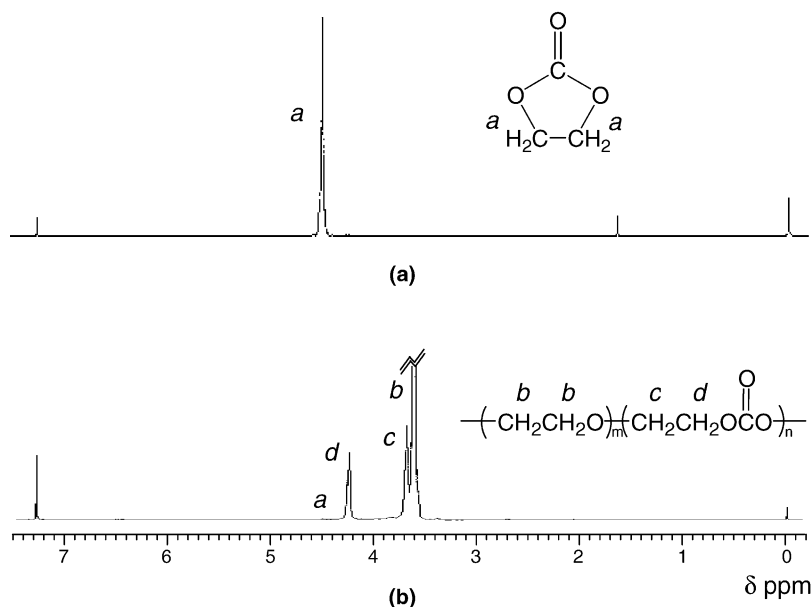


Fig. 1. ^1H NMR spectra of (a) EC and (b) P(EO-EC) in CDCl_3 with TMS as internal reference.

Fig. 2 shows the FT-IR spectra of EC and P(EO-EC) in the wavenumber range from 4000 to 400 cm^{-1} . The characteristic band of carbonate five-membered ring at around 1850 cm^{-1} was observed (Fig. 2(a)). This band was absent in the P(EO-EC) (Fig. 2(b)), which clearly demonstrates the occurrence of ring opening polymerization. The number average molecular weights and molecular weight distribution of P(EO-EC) were 1800 and 2.39 g mol^{-1} , respectively. An interesting feature of P(EO-EC) with a low T_g of ca. $-44\text{ }^\circ\text{C}$ was the lack of crystallinity, which showed no melting points in the thermal analytic traces. This is probably due to the random structure of ethylene oxide and ethylene carbonate units. We expect that the current limitation at temperature above $35\text{ }^\circ\text{C}$ due to the crystallization of polyether chains (e.g., PEO and poly(ethylene glycol) (PEG)) will be allevi-

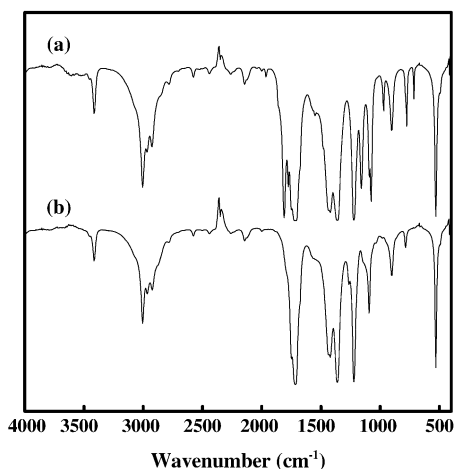


Fig. 2. FT-IR spectra of (a) EC and (b) P(EO-EC) at $25\text{ }^\circ\text{C}$.

ated by randomly introducing spacer groups in the polymer host. Therefore, this amorphous nature allows P(EO-EC) material to be successfully used as an ion-conducting polymer electrolyte because amorphous regions mainly contribute to the ionic conductivity.

3.2. Porosity, uptake, and morphology of porous membranes

In order to investigate the effects of annealing on porous membranes, they were annealed in a vacuum oven at $110\text{ }^\circ\text{C}$ for 2 h. The porosity and uptake of annealed porous membranes increased generally with increasing P(EO-EC) composition in the membranes and showed similar values with unannealed porous membranes (Table 1). This indicates that the introduction of viscous P(EO-EC) in the membranes results in the high porosity because the evaporation of non-solvent in flexible membranes is easier than that in rigid membranes. It also means that thermal annealing dose not have a great influence on porosity and uptake of porous membranes. On the other hand, despite the addition of a large amount of

Table 1
Porosity and uptake data of annealed and unannealed porous membranes

Samples	Porosity (%)		Uptake (%)	
	Annealed ^a	Unannealed	Annealed ^a	Unannealed
M-V10E0	54.2	54.3	36.1	36.4
M-V9E1	56.8	57.4	44.0	44.4
M-V8E2	58.9	59.1	48.7	48.2
M-V7E3	61.6	61.8	55.3	56.3
M-V6E4	64.2	64.6	61.1	61.3
M-V5E5	62.4	62.9	54.1	55.2

^a Porous membranes annealed at $110\text{ }^\circ\text{C}$ for 2 h.

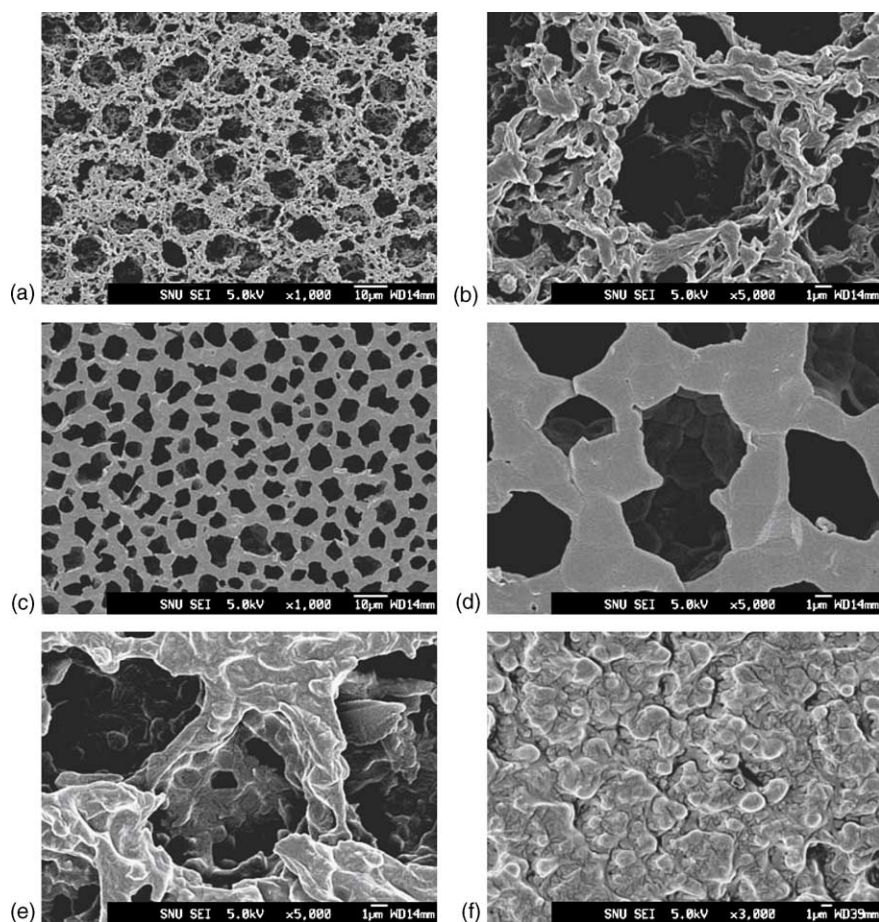


Fig. 3. Typical SEM micrographs of the surface of porous membranes and a polymer electrolyte: unannealed (a) M-V6E4 ($\times 1000$), (b) M-V6E4 ($\times 5000$); annealed (c) M-V6E4 ($\times 1000$), (d) M-V6E4 ($\times 5000$); (e) unannealed M-V5E5 ($\times 5000$); (f) E-V6E4 ($\times 3000$).

P(EO-EC), both annealed and unannealed M-V5E5 showed slightly low porosity compared to that of M-V6E4. Here, we should say that the porous membranes with above 50 wt% of P(EO-EC) in the membranes exhibited a sticky property, which means that it failed to obtain a self-supporting film.

Fig. 3 shows the surface SEM micrographs of a few porous membranes before and after thermal annealing. The membranes displayed a homogenous porous structure in the surface and a pore size in the range of 1–10 μm . Their surface pore size increased gradually with increase of P(EO-EC) composition in the membranes. Interestingly, annealed membranes (Fig. 3(c) and (d)) showed a highly ordered pore structure (i.e., honeycomb-like structure) and had smaller pores than unannealed membranes (Fig. 3(a) and (b)). In general, polymer chains in unannealed membranes are fixed as a form of the very loose structure. However, they are rearranged as a form of the very tight and highly ordered structure by thermal annealing, resulting in reduced pore size [21]. These structures may contribute to the substantial enhancement of mechanical properties. In Fig. 3(e), the image of M-V5E5 containing 50 wt% of P(EO-EC) showed a conglomeration

feature of P(EO-EC) near pores. It is thought that this conglomeration feature is a result of the inversion effect of host matrix from a P(VdF-HFP)-rich phase to a P(EO-EC)-rich phase, which consequently leads to the decrease of porosity. Fig. 3(f) shows that a viscous P(EO-EC)/LiCF₃SO₃ mixture is well filled into the pores of M-V6E4, thereby producing a solvent-free polymer electrolyte, E-V6E4. From these results, we could confirm that the morphology of the membranes can be tailored by modulating the relative polymer composition in the blend system and by thermal annealing as well as by other experimental factors such as the polymer concentration in the cast solution, the nature of the solvent, and the precipitation rate [22,23].

3.3. Mechanical properties of porous membranes

Tensile tests have generally been used to investigate the mechanical properties of polymer electrolytes. However, because porous membranes play effective roles as a supporter in polymer electrolytes, their mechanical properties are also an important factor that must be considered in the battery manufacturing process. In this study, stress–strain measurements

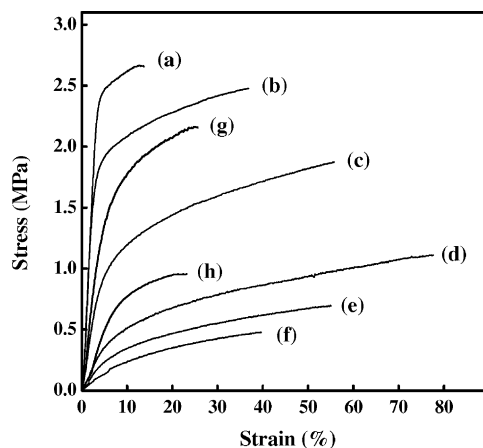


Fig. 4. Stress–strain curves of annealed and unannealed membranes with different P(EO-EC) compositions: unannealed (a) M-V10E0, (b) M-V9E1, (c) M-V8E2, (d) M-V7E3, (e) M-V6E4, (f) M-V5E5; annealed (g) M-V8E2, (h) M-V6E4.

were undertaken on dry porous membranes. Fig. 4 shows the stress–strain curve of annealed and unannealed membranes prepared by a phase inversion method. In the case of unannealed membranes, the M-V10E0 sample (Fig. 4(a)) prepared with pure P(VdF-HFP) had a maximum stress of 2.7 MPa, but had a low elongation-at-break value of ca. 13%. When the P(EO-EC) composition in the membranes increased, unannealed membranes showed a dramatic decrease in maximum stresses but a steady increase in elongation-at-break values, except M-V6E4 and M-V5E5. When the thermal annealing process was applied to porous membranes at 110 °C for 2 h, their tensile strength and modulus increased significantly (Fig. 4(g) and (h)). This is due to the highly ordered structure, as shown in Fig. 3. The increase of tensile modulus corresponding to this result is shown in Fig. 5. Overall, the thermal annealing technique can be said to be an efficient method for enhancing the mechanical properties, such as tensile strength and modulus of porous membranes.

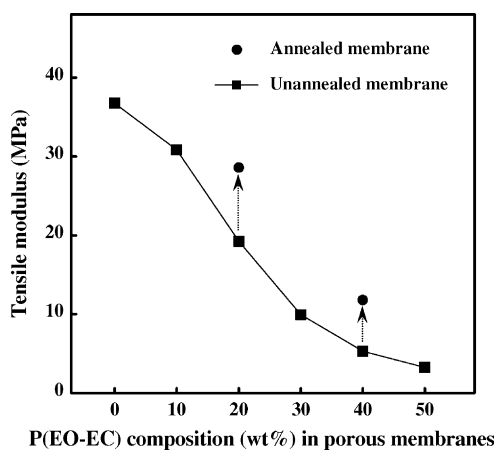


Fig. 5. Tensile modulus variations of annealed and unannealed membranes as a function of P(EO-EC) composition.

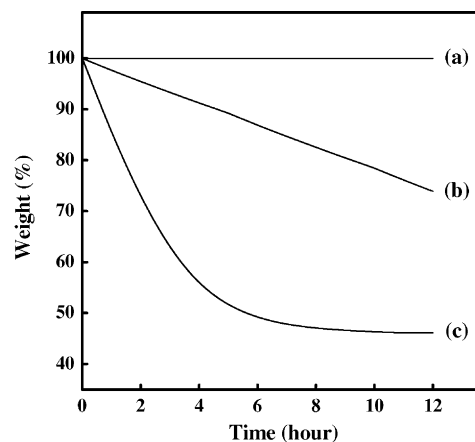


Fig. 6. Isothermal TGA curves for solvent-free and gel polymer electrolytes: (a) M-V6E4 filled with P(EO-EC)/LiCF₃SO₃ at 70 °C; (b) M-V6E4 filled with EC/PC/LiCF₃SO₃ mixture at 40 °C and (c) 70 °C.

3.4. Loss of electrolyte solution

Fig. 6 shows the isothermal TGA curves of polymer electrolytes. Gel polymer electrolytes were used as counterpart samples. The polymer electrolytes were heated at 40 and 70 °C for 12 h under a flow of argon, and the weight change was monitored as a function of time. As soon as it was exposed to a flowing atmosphere of argon, the weight of gel polymer electrolytes (Fig. 6(b) and (c)) consisting of EC/PC (1:1 by weight) and LiCF₃SO₃ as electrolyte solution started to decrease. We believe that this loss is attributed to the partial evaporation of the solvent mixture. After 10 h, gel polymer electrolytes lost 52 and 100% of the solvent confined in pores of porous membranes at 40 and 70 °C, respectively, whereas the loss of solvent-free polymer electrolytes (Fig. 6(a)) containing viscous P(EO-EC)/LiCF₃SO₃ did not occur even at 70 °C. It was reported [24] that the hybrid polymer electrolyte containing EC/PC and LiN(CF₃SO₂)₂ lost ca. 20 wt% of the electrolyte solution when thermally treated at 55 °C for 12 h, causing the ionic conductivity to decrease by 1–2 orders of magnitude. The result indicates that if the organic solvent is used in polymer electrolytes, some of them will be lost during preparation and storage of the gel polymer electrolytes, thereby resulting in deterioration of electrochemical performance. This drawback may be overcome by introducing a viscous ion-conducting polymer instead of organic solvent.

3.5. Ionic conductivity of solvent-free polymer electrolytes

Ionic conductivity of the polymer electrolytes was evaluated by ac impedance with a symmetric cell, having the polymer electrolyte sandwiched between two stainless steel (SS) electrodes. Fig. 7 shows the behavior of the ionic conductivity with the Li-salt concentration for E-V6E4 prepared by filling P(EO-EC)/LiCF₃SO₃ into the pores of the M-V6E4. The maximum conductivity was found at 1.5 mmol-LiCF₃SO₃/g-P(EO-EC). The conductivity of polymer electrolytes in-

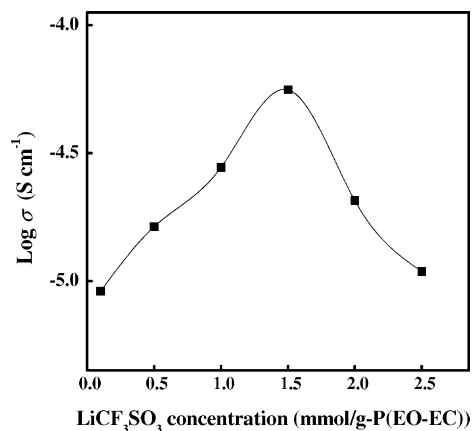


Fig. 7. The ionic conductivity vs. the lithium salt (LiCF_3SO_3) concentration for E-V6E4.

creased as the salt concentration increased up to 1.5 mmol- $\text{LiCF}_3\text{SO}_3/\text{g-P(EO-EC)}$, and after continuously adding the salt, the conductivity began to decrease. It was reported [25] that the ionic conductivity increased initially with increasing salt concentration as the number of charge carriers increased, but at higher salt concentration, the ionic conductivity was observed to decrease due to the increasing influence of ion pairs, ion triplets, and higher ion aggregations that reduces the overall mobility and number of effective charge carriers. This behavior is also similarly observable in polymer electrolytes that are dependent on salt concentration [26,27]. Thus, the optimum salt concentration of 1.5 mmol- $\text{LiCF}_3\text{SO}_3/\text{g-P(EO-EC)}$ was used for all subsequent series of measurements in this study. The ionic conductivity changes of the polymer electrolytes as a function of P(EO-EC) contents (i.e., P(EO-EC) uptake) confined in pores of unannealed porous membranes at various temperatures are shown in Fig. 8. The conductivity gradually increases with increasing P(EO-EC) content. This is related to the enhanced ion mobility and the increased number of charge carriers, which in turn is due to the addition of a large amount of P(EO-EC) content. Fig. 9 describes the Arrhenius plots of the polymer electrolytes based

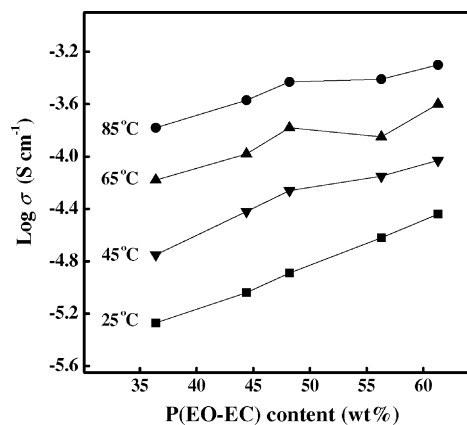


Fig. 8. The ionic conductivity of polymer electrolytes as a function of P(EO-EC) content at various temperatures.

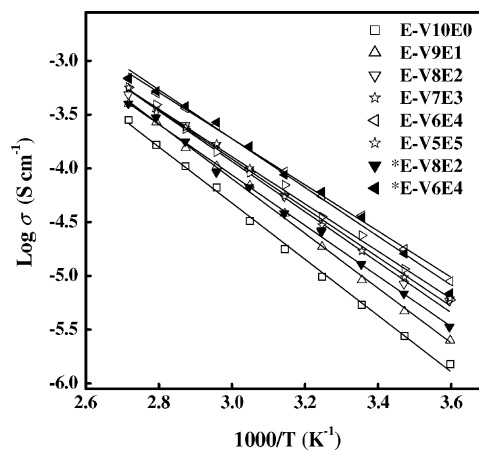


Fig. 9. Temperature dependence of ionic conductivity for polymer electrolytes. Data were fitted using the Arrhenius equation (solid lines). Asterisks mean the polymer electrolytes prepared using annealed porous membranes.

on annealed and unannealed membranes. Interestingly, even though there was a slight curvature in some of the plots, all the polymer electrolytes showed a linear enhancement of the ionic conductivity when the temperature was increased, but much less than that observed in similar plots for conventional SPEs. This behavior is known as Arrhenius behavior. This means that the ion conduction mechanism of these polymer electrolytes was not due to the dynamic configuration of the polymer matrix but rather due to the conduction path that was formed by filling the pores of porous membranes with P(EO-EC)/ LiCF_3SO_3 [28]. On the other hand, the conductivity of E-V6E4 based on unannealed M-V6E4 having the highest P(EO-EC) content was $3.7 \times 10^{-5} \text{ S cm}^{-1}$ at room temperature, which is similar to that ($3.5 \times 10^{-5} \text{ S cm}^{-1}$) of polymer electrolytes based on annealed M-V6E4 (Table 2) and these values are still lower than that of most gel systems. It is worthy to note that this value is higher compared to the prototype SPEs [29,30]. Furthermore, ionic conductivity of these systems was much higher than that of P(VdF-HFP)/P(EO-EC) blend systems complexed with LiCF_3SO_3 by 1–2 orders of magnitude, indicating that Li-ions had very high mobility in pores of porous membranes.

The slope of the Arrhenius plots is related to the activation energy, E_a , for ion transport. Thus, E_a can be determined by

Table 2
The ionic conductivity and activation energy data for polymer electrolytes based on annealed and unannealed porous membranes

Samples	$\sigma (\text{S cm}^{-1})$ at 25 °C		$E_a (\text{kJ mol}^{-1})$	
	Annealed ^a	Unannealed	Annealed ^a	Unannealed
E-V10E0		5.4×10^{-6}		50.1
E-V9E1		9.2×10^{-6}		48.7
E-V8E2	1.3×10^{-5}	1.3×10^{-5}	45.0	45.2
E-V7E3		1.7×10^{-5}		42.2
E-V6E4	3.5×10^{-5}	3.7×10^{-5}	43.1	41.2
E-V5E5		2.4×10^{-5}		43.7

^a Polymer electrolytes prepared using annealed porous membranes.

Arrhenius equation

$$\sigma = \sigma_0 \exp\left(-\frac{E_a}{RT}\right) \quad (6)$$

where σ is the ionic conductivity, σ_0 is a constant, E_a is the activation energy, R is the gas constant, and T is the temperature. E_a values of all polymer electrolytes covered the range of 41–50 kJ mol⁻¹ and they decreased with increasing P(EO-EC) content, giving a lowered temperature dependence of conductivity. This underlines the fact that polymer electrolytes with a large amount of P(EO-EC) content can have the advantages of low temperature dependence and consequent uniform response over a wide temperature range in practical applications.

4. Conclusions

The P(EO-EC) copolymer containing carbonate groups randomly linked by ether moieties was synthesized with EC and used to prepare both a porous membrane and an electrolyte mixture. The addition of P(EO-EC) to P(VdF-HFP) contributed to flexibility and high porosity, but led to a decrease in the mechanical strength. Porous membranes with enhanced mechanical strength and high porosity were successfully prepared by thermal annealing at 110 °C for 2 h. This was due to the formation of the highly ordered pore structure and small pores in porous structure by annealing. Solvent-free polymer electrolytes were fabricated by filling porous membranes with viscous P(EO-EC) complexed with LiCF₃SO₃, which plays an effective role as an ion conductor. The ionic conductivity of the polymer electrolyte based on an annealed membrane reached 3.5 × 10⁻⁵ S cm⁻¹ at room temperature, which was a similar to that (3.7 × 10⁻⁵ S cm⁻¹) of the polymer electrolyte based on an unannealed membrane. From these results, we suggest that solvent-free polymer electrolytes filled with a viscous polymer could be a promising candidate in rechargeable lithium batteries and this new approach may offer the opportunity to design a polymer electrolyte with improved performance.

Acknowledgement

The authors are grateful to the Korea Science and Engineering Foundation (KOSEF) for the support of this study

through Hyperstructured Organic Materials Research Center (HOMRC).

References

- [1] F. Croce, G.B. Appetecchi, L. Persi, B. Scrosati, *Nature* 394 (1998) 456.
- [2] R. Ulrich, J.W. Zwanziger, S.M. De Paul, A. Reiche, H. Leuninger, H.W. Spiess, U. Wiesner, *Adv. Mater.* 14 (2002) 1134.
- [3] Z. Gadjourova, Y.G. Andrew, D.P. Tunstall, P.G. Bruce, *Nature* 412 (2001) 520.
- [4] D.W. Kim, *J. Power Sources* 55 (1998) 7.
- [5] G.B. Appetecchi, F. Croce, G. Dautzenberg, M. Mastragostino, F. Ronci, B. Scrosati, F. Soavi, A. Zanelli, F. Alessandrini, P.P. Prosini, *J. Electrochem. Soc.* 145 (1998) 4126.
- [6] C. Berthier, W. Gorecki, M. Minier, M.B. Armand, J.M. Chabagno, P. Rigaud, *Solid State Ionics* 11 (1983) 91.
- [7] A. Bouridah, F. Dalard, D. Deroo, H. Cheradame, J.F. Le Nest, *Solid State Ionics* 15 (1985) 233.
- [8] W. Wiczcerek, J.R. Stevens, *J. Phys. Chem. B* 101 (1997) 1529.
- [9] M. Kovac, M. Gaberscek, J. Grdadolnik, *Electrochim. Acta* 44 (1998) 863.
- [10] Y.-T. Kim, E.S. Smotkin, *Solid State Ionics* 149 (2002) 29.
- [11] R. Frech, S. Chintapalli, *Solid State Ionics* 85 (1996) 61.
- [12] Y. Liu, J.Y. Lee, L. Hong, *J. Power Sources* 129 (2004) 303.
- [13] M.A.K.L. Dissanayake, P.A.R.D. Jayathilaka, R.S.P. Bokalawala, I. Albinsson, B.-E. Mellander, *J. Power Sources* 119–121 (2003) 409.
- [14] J.-H. Ahn, G.X. Wang, H.K. Liu, S.X. Dou, *J. Power Sources* 119–121 (2003) 422.
- [15] G.B. Appetecchi, F. Croce, M. Mastragostino, B. Scrosati, F. Soavi, F. Zanelli, *J. Electrochem. Soc.* 145 (1998) 4133.
- [16] J.-C. Lee, *Macromolecules* 33 (2000) 1618.
- [17] W.-T. Whang, C.L. Lu, *J. Appl. Polym. Sci.* 56 (1995) 1635.
- [18] K. Soga, S. Hosada, Y. Tazuke, S. Ikeda, *J. Polym. Sci., Polym. Lett. Ed.* 14 (1976) 161.
- [19] L. Vogdanis, W. Heitz, *Makromol. Chem., Rapid Commun.* 7 (1986) 543.
- [20] R.F. Storey, D.C. Hoffman, *Macromolecules* 25 (1992) 5369.
- [21] I.-C. Kim, H.-G. Yun, K.-H. Lee, *J. Membr. Sci.* 199 (2002) 75.
- [22] H. Strathmann, K. Kock, *Desalination* 21 (1977) 241.
- [23] A. Bottino, B. Camera-Roda, G. Capannelli, S. Munari, *J. Membr. Sci.* 57 (1991) 1.
- [24] E. Quartarone, M. Brusa, P. Mustarelli, C. Tomasi, A. Magistris, *Electrochim. Acta* 44 (1998) 677.
- [25] J.R. MacCallum, A.S. Tomlin, C.A. Vincent, *Eur. Polym. J.* 22 (1986) 787.
- [26] J.M.G. Cowie, G.H. Spence, *Solid State Ionics* 109 (1998) 139.
- [27] M. Shibata, T. Kobayashi, R. Yosomiya, M. Seki, *Eur. Polym. J.* 36 (2000) 485.
- [28] S.H. Kim, J.K. Choi, Y.C. Bae, *J. Appl. Polym. Sci.* 81 (2001) 948.
- [29] M.M.E. Jacob, S.R.S. Prabaharan, S. Radhakrishna, *Solid State Ionics* 104 (1997) 267.
- [30] S. Rajendran, R. Kannan, O. Mahendran, *J. Power Sources* 96 (2001) 406.